

Mapping Urban Thermal Environment & Climate-Related EV Activity

Content

1. Introduction.....	2
1.1 Background.....	2
1.2 Topic Identification.....	2
2. Literature Review.....	3
3. Data Collection.....	3
4. Methodology and Result.....	4
4.1 Mapping and Measuring Density Distribution Using H3 Hexagonal Hierarchical Geospatial Indexing System.....	4
4.2 Mapping and Measuring Green Space Data Density Distribution from OpenStreetMap.....	6
4.3 Mapping and Measuring Land Surface Temperature Data Distribution using Google Earth Engine.....	9
4.4 Mapping and Measuring the Distribution of EVs related data.....	12
4.4.1 Electric Vehicle Station.....	12
4.4.2 Electric Vehicle Demand.....	15
4.4.3 CO ₂ Emission by Electric Vehicle.....	17
4.5 Mapping and Measuring Urban Structure Factor Using Osmnx.....	20
4.5.1 Buildings Height Distribution.....	20
4.5.2 Road Network Structure.....	22
5. Correlation Analysis.....	25
5.1 Green Space and Urban Environment.....	26
5.2 Electric Vehicle Infrastructure.....	26
5.3 Urban Density and Emissions.....	27
5.4 Thermal Environment.....	27
6. Principal Component Analysis.....	27
6.1 Cumulative Explained Variance by PCA Components.....	27
6.2 PCA Loadings and Component Interpretation.....	28
6.3 Explained Variance Ratio.....	29
6.4 Elbow Method for Optimal Number of Components.....	30
6.5 Cluster Analysis on PCA Components.....	31
6.6 Spatial Distribution of Clusters.....	32
7.2 Policy Making.....	33
7.3 Urban Planning.....	34
8. Conclusion and Next Step.....	34
8.2 Next Step.....	34
8.2.1 Racial Density Distribution.....	34
8.2.2 Index Map.....	35
8.2.3 Deliverable.....	36
Reference.....	37

1. Introduction

1.1 Background

Extreme heat is the number-one climate killer in the U.S., accounting for more deaths than sea level rise, flooding, drought, and other impacts. Reducing CO₂ emissions is a growing challenge for the transport sector. Transportation produces roughly 23 percent of the global CO₂ emissions from fuel combustion. Our primary concern is how can we boost EV usage and equality to boost sustainable urban development towards climate change. We are interested in how the different regions of a city can vary according to different urban environments in Climate Change (LST & CO₂). Points of interest (POI) can be Land Surface Temperature (LST) and Carbon dioxide (CO₂). A city can have different building types, population density, race density, green space density, and so forth. For now, we selected the following metrics to measure the relationship between POIs like LST, Urban EV CO₂ Emission, and Urban Structure.

1.2 Topic Identification

To address these disparities and promote a sustainable city, I'm interested in several metrics that might serve as indicators interacting with climate change and EVs. So this study aims to use the exploratory data analysis (EDA) method to explore the relationship among selected variables. The primary concern is how to boost EV usage and equality to boost sustainable urban development towards climate change. We are interested in how the different regions of a city can vary according to different urban environments in Climate Change. Points of interest (POI) can be Land Surface Temperature (LST) and Carbon dioxide (CO₂). A city can have different building types, population density, race density, green space density, and so forth. For now, we selected the following metrics to measure the relationship between POIs like LST & Urban EV CO₂:

- Land Surface Temperature
- Electric Vehicle Station Density
- Electric Vehicle Demand Density
- CO₂ Emission Distribution from Electric Vehicles
- Green Space Density (Location-based)
- Urban Street Typology Structure (Network Centrality, street density, building height, etc)
- Race Density

2. Literature Review

The combined effect of climate change and the urban heat island challenges the living conditions in cities, with consequences on human health, the economy and ecosystems ([Revi et al., 2014](#)). The UHI intensity is strongly related both to external influences (e.g., climate, weather, and season) and to the intrinsic characteristics of a city (e.g., city size, building density, and land-use distribution) ([Oke 1982](#)). Several papers use linear regression analysis to study the relationship between different Urban Heat Island (UHI) indicators. Typically, these methods are used to develop composite indicators that quantify access by combining a number of individual indicators. [Lin et al. \(2017\)](#) investigate the impact of pocket parks on UHI intensity and Floor Area Ratio (FAR), building density, and Tree Cover Ratio (TCR) as urban planning indicators can significantly decrease UHI. [Kammuang-Lue et al. 2015](#) focused on how population density, building density, and traffic density influence UHII during different seasons. Husni et al. 2022 improved the UHI model for predicting how traffic congestion contributes to the UHI effect. [Yin et al. 2018](#) emphasized that urban form metrics, especially building density, are critical for UHI mitigation efforts using spatial regression. [Lu et al. 2012](#) utilized regression Analysis of the Relationship between four canopy characteristics: impermeable rate (IR), building density (BD), water body percentage (WBP), and planting rate (PR) with UHI.

Recently, with the implementation of policies related to carbon emission reduction goals, cities have been asked to take an active role in mitigating their contribution to global warming and associated climate change by reducing their CO₂ emissions ([Hsu et al., 2020](#)). Such policies are motivated by the long-recognized environmental benefits of EVs ([Hardman et al., 2017](#)) which include their positive impact on air quality (Liang et al., 2019) and CO₂ emissions ([Wolfram and Lutsey, 2016](#)). [Mussetti et al. \(2022\)](#) indicated that the full fleet electrification (FE) produces a reduction in near-surface air temperature, and is substantial during the morning traffic peak (up to 0.6°C). Therefore, the adoption of electric vehicles is expected to lead to a decrease in the emission of heat from vehicle exhausts within city settings, enhancing the thermal comfort and environmental quality of urban areas.

3. Data Collection

The data utilized for this mapping analysis combines census-level social demographic data, electrical vehicle trip origin-destination (OD) trajectory data, Google Earth engine urban land surface temperature data, and open street network data. The EV data is connected to geospatial data relating to open street map points of interest. All data was collected online. The sources of data include:

- New York City census county boundary shapefile data ([NYC Open Data - \(cityofnewyork.us\)](#))
- Replica EVs trip OD trajectory data (<https://www.replicahq.com/>)

- Bay Area Counties shapefile data: Bay Area Counties | DataSF | City and County of San Francisco (sfgov.org)
- MOD11A1.061 Terra Land Surface Temperature and Emissivity Daily Global 1km data ([LP DAAC - MOD11A1 \(usgs.gov\)](http://LP DAAC - MOD11A1 (usgs.gov)))
- U.S. Department of Energy's Alternative Fuels Data Center Electric Vehicle Charging Station ([Alternative Fuels Data Center: Maps and Data \(energy.gov\)](http://Alternative Fuels Data Center: Maps and Data (energy.gov)))
- New York State boundary shapefile data ([Index of /geo/tiger/GENZ2016 \(census.gov\)](http://Index of /geo/tiger/GENZ2016 (census.gov)))
- New York City census tract and block group shapefile data ([Understanding Geographic Identifiers \(GEOIDs\) \(census.gov\)](http://Understanding Geographic Identifiers (GEOIDs) (census.gov)))
- Open Street Map: for data on the locations of green space, and driving roads (<https://osmnx.readthedocs.io/en/stable/>)

Table 1. Data Source Table

Variables/ illustration	Region boundary	LST °C	EV Station	EV Demand	EV CO2	Green Space	Building Footprint	Urban Structure
Data Source	U.S. Census Bureau	NASA LP DAAC	U.S. Depart ment of Energy	Replica	Replica	Open Street Network	NY Open Data	Open Street Network
Data Type	.SHP	.TIF	.CSV	.CSV	.CSV	.JSON	.SHP	GRAPH

4. Methodology and Result

4.1 Mapping and Measuring Density Distribution Using H3 Hexagonal Hierarchical Geospatial Indexing System

H3 is a geospatial indexing system using a hexagonal grid that can be (approximately) subdivided into finer and finer hexagonal grids, combining the benefits of a hexagonal grid with S2's hierarchical subdivisions. To better understand the mapping results, H3 hexagonal grids were employed in this study to visualize the spatial distribution of urban thermal environment and climate-related electric vehicle (EV) activity. The choice of a hexagonal grid system over traditional square grids was motivated by several key advantages:

- Hexagonal cells maintain an equal area across the study region, ensuring that density values are not distorted by varying cell sizes. This property is crucial when mapping thermal and EV activity patterns, as it allows for an accurate representation of the underlying phenomena.
- The hexagonal grid's improved adjacency, with each cell having six equidistant neighbors, facilitates spatial analysis tasks such as interpolation and clustering, enabling more robust modeling of thermal dynamics and EV usage patterns.
- The hexagonal grid mitigates sampling bias associated with square grids, providing more uniform coverage of the study area and reducing the influence of grid orientation on the analysis results.
- The hexagonal grid's visual appeal and ability to create visually appealing patterns and gradients enhance the communication and interpretation of the spatial patterns observed in the urban thermal environment and climate-related EV activity.

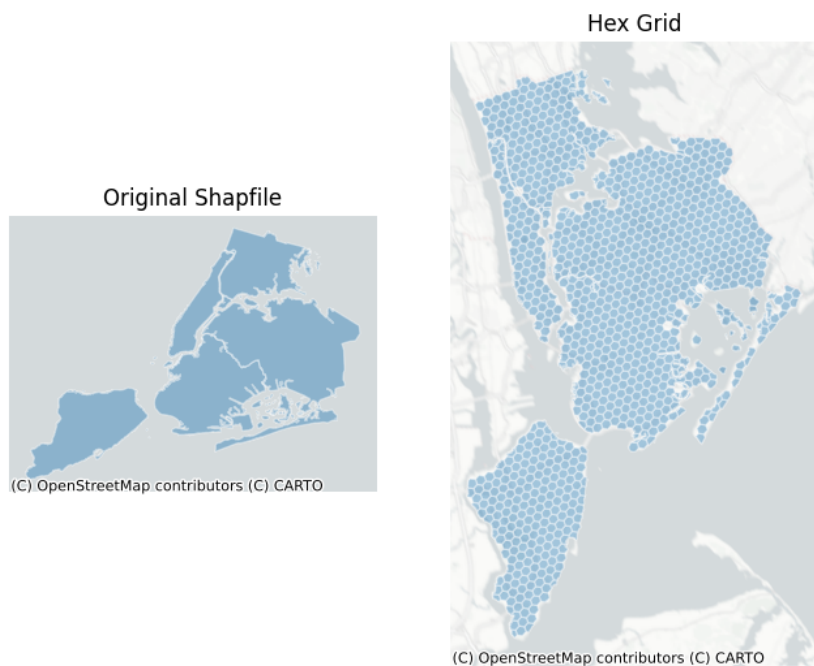


Figure 1. Comparative New York City H3 Hexagonal Grid Plot

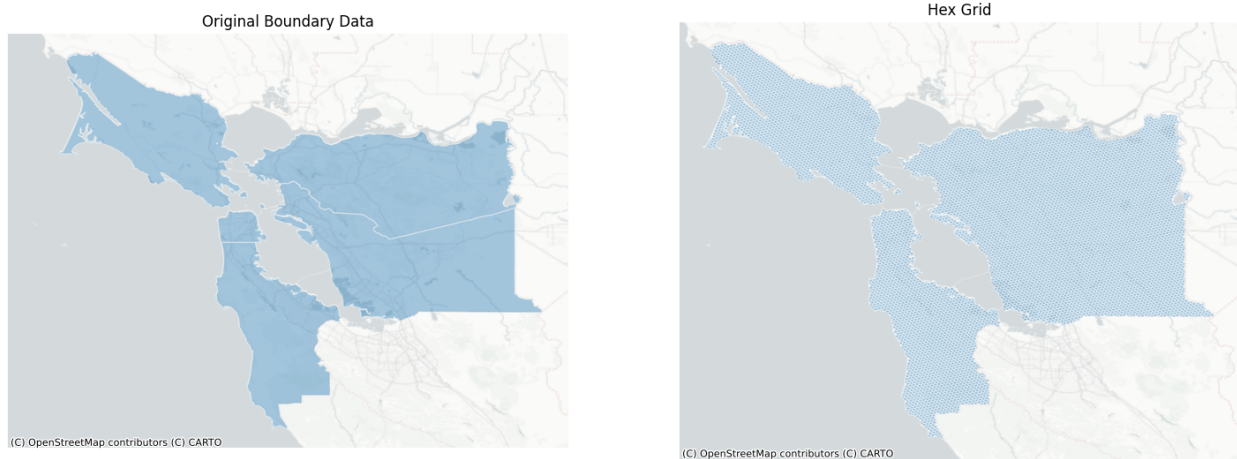


Figure 2. Comparative San Francisco-Oakland-Berkeley CBSA H3 Hexagonal Grid Plot

By leveraging the advantages of the hexagonal grid system, this study aimed to provide a comprehensive and accurate representation of the interplay between urban thermal dynamics and EV usage, informing sustainable urban planning and transportation strategies.

4.2 Mapping and Measuring Green Space Data Density Distribution from OpenStreetMap

The locations of leisure parks in New York City were accessed from the [OpenStreetMap \(OSM\)](#) data using the [osmnx](#) library. OSM is a collaborative project that provides open-source geographic data, including information on parks and recreational areas. The following methodology was followed to estimate green space (leisure parks) density in New York City for each hexagon:

1) Filter the green space data

The data was filtered borough-wise to ensure a comprehensive coverage of the study area. Smaller parks with an area of less than 500,000 square meters were excluded from the analysis. This filtering step was performed to focus on larger, more significant green spaces that are likely to have a greater impact on the urban thermal environment and climate-related activities. Smaller parks may not provide sufficient greenery or recreational space to significantly influence these factors.

2) Define the study area boundary

The boundary of the study area (New York City) was defined using a spatial data file (e.g., a shapefile or GeoJSON) containing the administrative boundaries of the city.

3) Set the H3 resolution

The desired resolution for the H3 hexagonal grid was set to 8, which determines the size of the hexagonal cells. A higher resolution (larger number) results in smaller hexagon sizes, allowing for a more granular

analysis but also increasing computational complexity. The chosen resolution of 8 strikes a balance between spatial detail and computational efficiency for the study area.

4) Create a GeoDataFrame with H3 hexagons

A GeoDataFrame with H3 hexagons covering the study area was created using the `h3.polyfill` function from the `h3` library. This function generates a set of hexagonal indexes (H3 addresses) that cover the specified geometry (in this case, the New York City boundary). The `h3.h3_to_geo_boundary` function was then used to convert the H3 addresses to Polygon geometries, which were stored in the GeoDataFrame.

5) Spatial join between hexagons and parks

A spatial join was performed between the GeoDataFrame containing the H3 hexagons and the leisure parks data. This operation assigns each park to its respective hexagon(s) based on their spatial intersection. The resulting GeoDataFrame contains both the hexagon geometries and the associated park information.

6) Calculate green space density

For each hexagon, the green space density was calculated by computing the total area of parks within the hexagon and dividing it by the total area of the hexagon. This metric provides a normalized measure of the green space coverage within each hexagonal cell, enabling meaningful comparisons across different areas.

7) Visualize the green space density distribution

The green space density distribution was visualized using a choropleth map, with the hexagons colored based on their corresponding green space density values. This visualization technique allows for an effective communication of the spatial patterns and variations in green space density across the study area.



Figure 3. Distribution of Green Open Spaces in New York City and Surrounding Counties

Figure 3 shows the distribution of green open spaces, represented by the green-colored areas, across the New York City region and its surrounding counties. This map provides an overview of the spatial distribution of parks, recreational areas, and other green spaces within the study area. It serves as the initial input data for the analysis, highlighting the locations and extent of these green spaces.

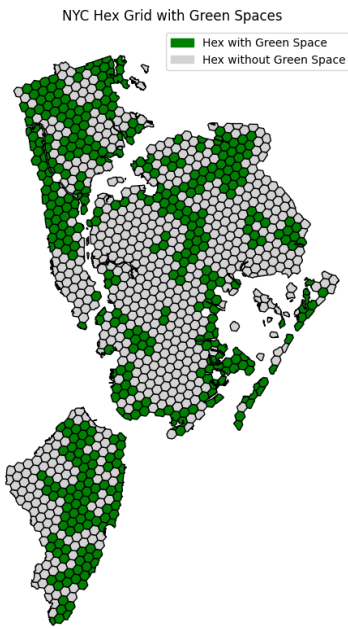


Figure 4. H3 Hexagonal Grid Representation of Green Space Distribution in New York City

Figure 4 presents the results of the methodology described in the research paper, where a hexagonal grid system (H3) has been applied to visualize the distribution of green spaces across New York City. The hexagonal grid cells are colored based on the presence or absence of green spaces within their boundaries. The green hexagons in Figure 4 indicate cells that contain at least a portion of a green space, such as a park or recreational area. These cells are considered to have a significant presence of green spaces within their boundaries. On the other hand, the gray hexagons represent cells that do not overlap with any green spaces, indicating a lack of green spaces within those particular areas. Each hexagonal cell covers an equal area, ensuring that the density or presence of green spaces is not distorted by varying cell sizes. The hexagonal grid structure allows for better representation of spatial relationships and adjacencies, facilitating more accurate analysis of spatial patterns and clustering.

4.3 Mapping and Measuring Land Surface Temperature Data Distribution using Google Earth Engine

To analyze the urban thermal environment and its potential impact on climate-related electric vehicle (EV) activity, land surface temperature (LST) data was incorporated into the study. The LST data provides valuable information about the spatial distribution of surface temperatures across the study area, which can influence factors such as urban heat island effects and energy consumption patterns related to EV usage. The LST data was obtained from the Moderate Resolution Imaging Spectroradiometer (MODIS) instrument aboard the Terra and Aqua satellites. Specifically, the MOD11A1 product, which provides daily land surface temperature and emissivity values at a 1-kilometer spatial resolution, was utilized. The data retrieval and processing were facilitated through the Google Earth Engine (GEE) platform, a cloud-based geospatial analysis platform that provides access to a vast repository of remote sensing data and computational resources. The following steps were taken to measure the LST data density distribution using GEE:

1) Authentication and Initialization

The script authenticated and initialized the GEE Python API, establishing a connection to the GEE environment.

2) Area of Interest Definition

A rectangular area of interest (AOI) covering New York City was defined using the geographic coordinates -74.2591, 40.4774, -73.7004, 40.9176.

3) Data Filtering and Processing

The MODIS LST data for daytime temperatures during Spring 2023 was accessed from the GEE data catalog. The data was filtered by date range and the defined AOI and the LST_Day_1km band were selected. The mean LST value across the filtered images was calculated, and the temperature values were converted from Kelvin to Celsius.

4) Data Clipping and Scaling

The processed LST data was clipped to the bounds of New York City to focus the analysis on the study area. Additionally, the scale of the data was adjusted to reduce the image resolution and size, facilitating more efficient data handling and processing.

5) Data Download and Alignment

A download URL for the clipped GeoTIFF image was generated, and the data was retrieved using the requests library in Python. The downloaded LST data was then loaded, and its coordinate reference system (CRS) was aligned with the H3 hexagonal grid vector data.

6) LST Sampling at Hexagon Centroids

For each hexagon in the H3 grid, the centroid was calculated, and the corresponding LST value was sampled from the raster data at the centroid location. This process assigned an LST value to each hexagonal cell, enabling the analysis of the LST density distribution across the study area.

7) Visualization

The LST raster data and the hexagonal grid with sampled LST values were visualized using appropriate colormaps and choropleth maps, respectively. These visualizations aided in the interpretation and communication of the spatial patterns in the urban thermal environment.

```
var dataset = ee.ImageCollection('MODIS/061/MOD11A2')
  .filter(ee.Filter.date('2023-03-01', '2023-05-31'));
var landSurfaceTemperature = dataset.select('LST_Day_1km');
var landSurfaceTemperatureVis = {
  min: 14000.0,
  max: 16000.0,
  palette: [
    '040274', '040281', '0502a3', '0502b8', '0502ce', '0502e6',
    '0602ff', '235cb1', '307ef3', '269db1', '30c8e2', '32d3ef',
    '3be285', '3ff38f', '86e26f', '3ae237', 'b5e22e', 'd6e21f',
    'fff705', 'ffd611', 'ffb613', 'ff8b13', 'ff6e08', 'ff500d',
    'ff0000', 'de0101', 'c21301', 'a71001', '911003'
  ],
};
Map.setCenter(6.746, 46.529, 2);
Map.addLayer(
  landSurfaceTemperature, landSurfaceTemperatureVis,
  'Land Surface Temperature');
```

Figure 5. Google Earth Engine Code Editor Script

Figure 5 is the code script for processing Land Surface Temperature in the 2023 spring season.

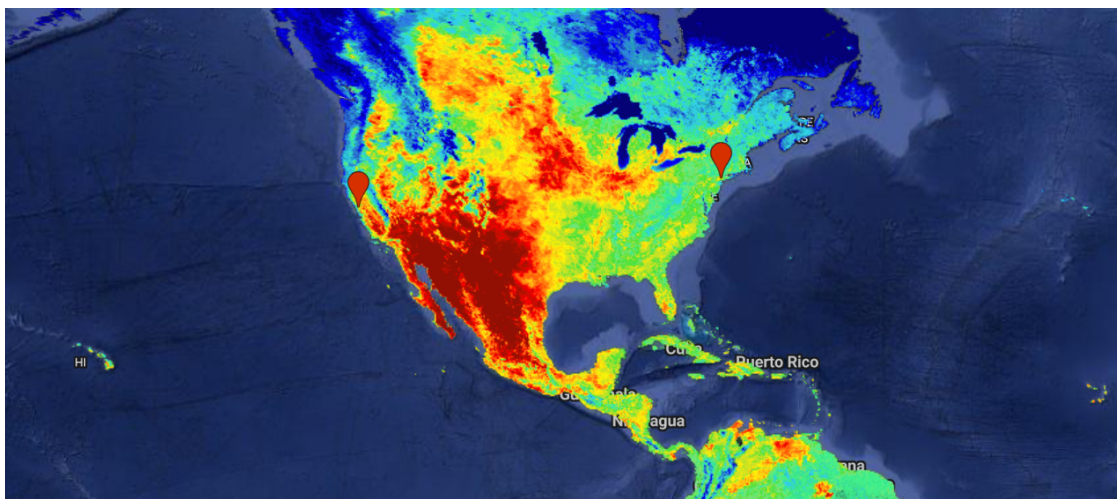


Figure 6. 2023 Spring Land Surface Temperature in the United States

Figure 6 demonstrates the visualization result of the Google Earth Engine code.

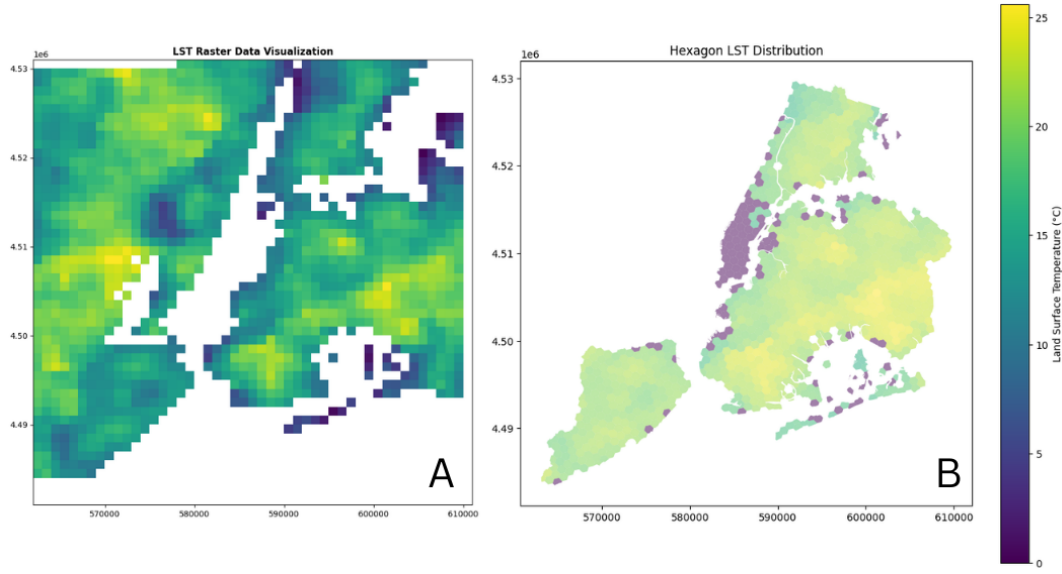


Figure 7. Comparative Visualization of LST in NYC: Raster and Hexagonal Grid Analysis

Figure 7 is the Comparative Visualization of LST in NYC: Raster and Hexagonal Grid Analysis. Panel A presents the LST data in a raster format highlighting the pixel-by-pixel temperature variations across the cityscape. Panel B displays the same LST data applied to a hexagonal grid, where each hexagon represents the mean temperature within its area, calculated from the centroid LST value. Both panels utilize a consistent color scale ranging from 5°C (purple) to 25°C (yellow), facilitating direct comparison between the granular raster data and the aggregated hexagonal representation.

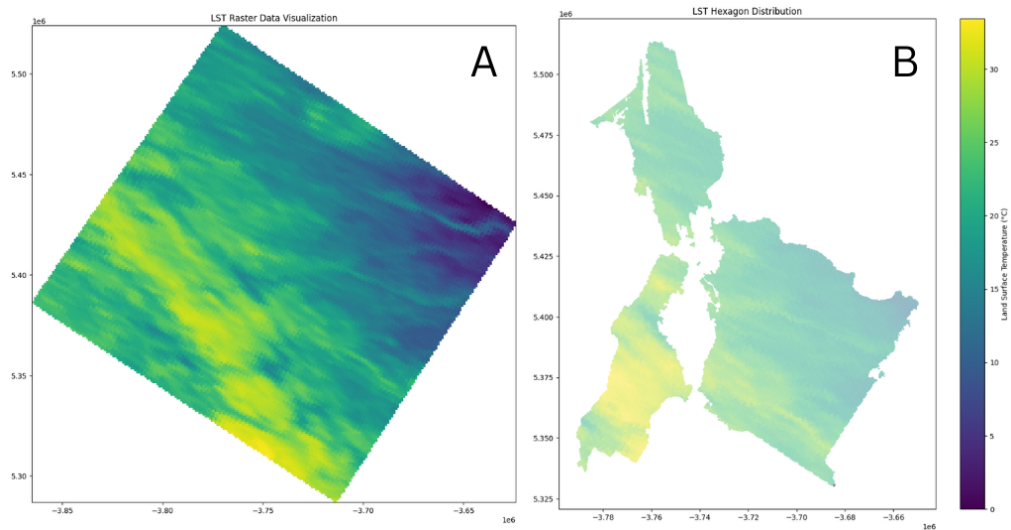


Figure 8. Comparative Visualization of LST in Selected Area: Raster and Hexagonal Grid Analysis

Figure 8 displays two methods of visualizing Land Surface Temperature (LST) data over a geographic region. This figure exemplifies the application of two spatial data visualization techniques to represent land surface temperature (LST) for a geographical region, useful in assessing environmental and climatic conditions. Panel A employs a raster-based approach to display LST data, where the fine granularity of the data is evident through the detailed color transitions, highlighting micro-climatic variations across the terrain. This method is particularly valuable for identifying specific hotspots and cooler areas, facilitating detailed analyses of localized climate behavior and its potential impacts on local ecosystems and urban heat dynamics. Panel B, conversely, utilizes a hexagonal grid to aggregate and simplify the LST data, reducing the spatial resolution but enhancing the ability to discern broader regional temperature patterns. This approach helps in understanding larger-scale climatic trends and is advantageous for strategic planning and policy-making where detailed data may be less critical than overall trends. Both panels are crucial for comprehensive environmental analysis, offering insights into the spatial distribution of temperatures which can influence ecological balances, human health, and urban planning. Such visualizations are instrumental in environmental research, providing a basis for comparative studies of different data aggregation techniques and their implications for interpreting climatic data in relation to environmental and urban planning policies. By leveraging the Google Earth Engine platform and its integration with Python, this study could efficiently access, process, and analyze the MODIS LST data, a crucial component in understanding the urban thermal environment and its potential influence on climate-related EV activity in New York City.

4.4 Mapping and Measuring the Distribution of EVs related data

4.4.1 Electric Vehicle Station

The EV charging station data included attributes such as station ID, location coordinates, operational dates, access times, connector types, facility type, pricing, and workplace charging availability. These attributes were refined to focus on geographic coordinates and identifiers, ensuring that all entries had valid latitude and longitude for spatial analysis. The GIS data was processed to include only land areas by filtering out water bodies and selecting only the tracts within the five boroughs of New York City. The coordinate reference system (CRS) for all spatial data was standardized to EPSG:4326 for compatibility in spatial operations. The methodology involved several key steps:

1) Tools

The code integrates various Python libraries like requests, zipfile, io, pandas, geopandas, matplotlib, contextily, and folium to execute these tasks. The choice of libraries ensures a robust workflow capable of handling spatial data efficiently, from data manipulation to advanced visualization.

2) Data Preparation and Filtration

The initial dataset comprised shapefiles obtained from the U.S. Census Bureau, which included all census tracts for New York State. These files were filtered to retain only those tracts within the geographical boundaries of New York City's five boroughs, identified by their Federal Information Processing Standards (FIPS) codes. To ensure that the analysis was restricted to terrestrial regions, tracts containing water bodies (where ALAND is zero) were excluded.

3) Spatial Join to Identify Charging Stations

EV charging station data, sourced from the U.S. Department of Energy, included detailed information on the location and characteristics of each station. This dataset was processed to convert latitude and longitude information into geometrical points suitable for spatial operations. Both the EV station data and the census tract data were harmonized to the same Coordinate Reference System (CRS) to enable accurate spatial joins. Using GeoPandas' spatial join function to merge the EV data with the tract data to identify stations located within the boundaries of NYC tracts.

4) Hexagonal Grid Creation and Density Calculation

To analyze the density distribution of EV stations, a hexagonal grid was overlaid across the map of New York City. The grid was generated using the H3 library's geo-indexing capabilities, set to a resolution that balanced detail with computational efficiency. A second spatial join was executed to count the EV stations within each hexagon. Density was then calculated as the number of stations per square kilometer of each hexagon, allowing for a uniform measure of station distribution across the city.

5) Visualization

Visualization played a critical role in the interpretation and presentation of data. Initial scatter plots generated with Matplotlib illustrated the geographical spread of EV stations. For a more detailed analysis, choropleth maps were created using both Matplotlib for static displays and Folium for interactive mapping. These maps were color-coded to reflect the density of EV stations, with different shades indicating varying levels of station concentration. The interactive maps allowed users to explore data dynamically, providing insights into the spatial distribution of EV infrastructure relative to the urban layout.

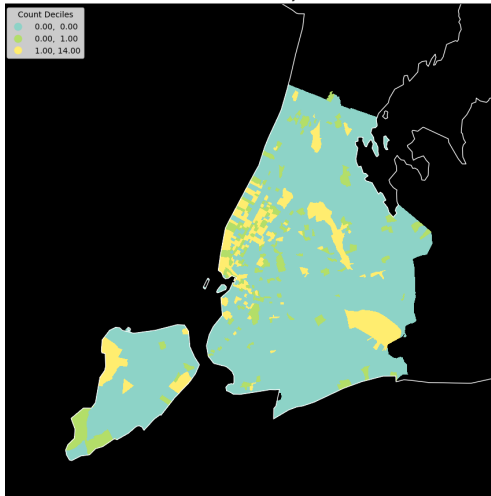


Figure 9. Density of Electric Vehicle (EV) Charging Stations in New York City

Figure 9 shows the density of EV charging stations per square kilometer across the Greater New York City area, depicted through a hexagonal grid. The color gradient from purple to green represents the density range from 0 to 28.31 stations per square kilometer, categorized into quartiles. This visualization aids in identifying areas with high and low infrastructure density, crucial for planning and policy-making in urban sustainability.

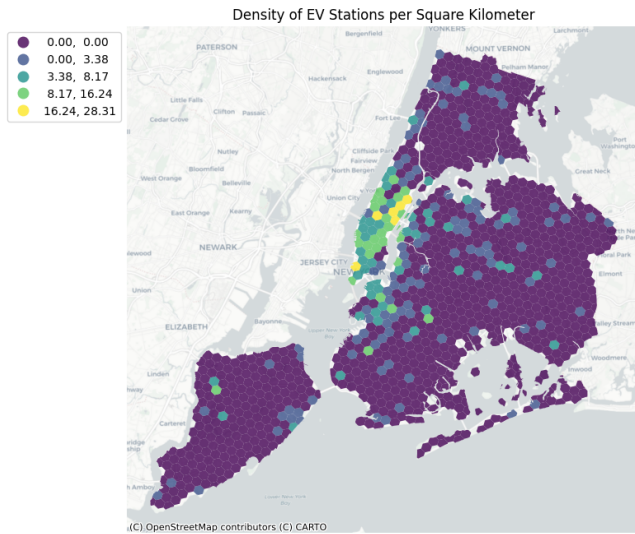


Figure 10. The density of EV Stations per Square Kilometer

Figure 10 employs a hexagonal grid to visualize the density of EV charging stations per square kilometer throughout New York City. The density ranges from 0 to 28.31 stations, with a color gradient from purple

(low density) to green (high density). This method provides a clear, structured representation of data that helps in identifying patterns of infrastructure distribution across different urban areas.

The map of EV charging station density in New York City reveals a strategic deployment of EV infrastructure. Areas with higher densities of EV stations often correspond to regions with higher population densities and greater urban heat island effects. This correlation suggests that the city is actively leveraging EV infrastructure as part of its climate adaptation strategy, aiming to reduce greenhouse gas emissions and potentially moderate local temperatures through decreased use of combustion engines. The analysis also indicates potential areas for further expansion of EV infrastructure, particularly in outer boroughs or less serviced neighborhoods, to ensure equitable access and further reduction of urban heat impacts. The densest concentrations appear in central urban regions, aligning with areas likely to experience significant urban heat island effects. These findings suggest that the more densely populated and potentially warmer areas of the city are being prioritized for EV infrastructure deployment, which supports the city's broader climate adaptation and sustainability strategies. The strategic placement of these stations not only promotes the use of electric vehicles but also potentially contributes to mitigating urban heat by reducing dependence on internal combustion vehicles. The methodology allowed for an insightful analysis of the spatial distribution and density of EV charging stations in New York City, highlighting areas of high and low availability. The use of hexagonal grids provided an innovative approach to spatial density analysis, offering a more uniform basis for comparison than traditional census tract methods. This analysis is crucial for urban planning and sustainability studies, as it provides a detailed view of infrastructure distribution relative to urban density and accessibility.

4.4.2 Electric Vehicle Demand

1) Data Sources and Processing

This section leverages data extracted from various sources to analyze the demand for electric vehicles (EVs) within New York City. The primary data comes from the NYC block shapefile, which includes geographical and demographical details necessary for this analysis. Further, EV-related emissions data is utilized to compare the environmental impact of different transportation modes, thereby highlighting the benefits of EVs.

2) Hexagonal Binning

The study uses a hexagonal binning approach to spatially aggregate and analyze EV-related data across New York City. This method helps in understanding the distribution density of EVs and identifying hotspots of EV activity. Each block in the city is assigned to a hexagonal cell, and data points within each hex are aggregated to measure EV density. The hexagonal grid can provide a clear visual representation of

areas with high EV activity demand, allowing for a straightforward interpretation of urban zones with increased EV usage. The use of color gradients in the plots highlights areas of different EV densities, providing insights into potential areas for infrastructure development such as EV charging stations.

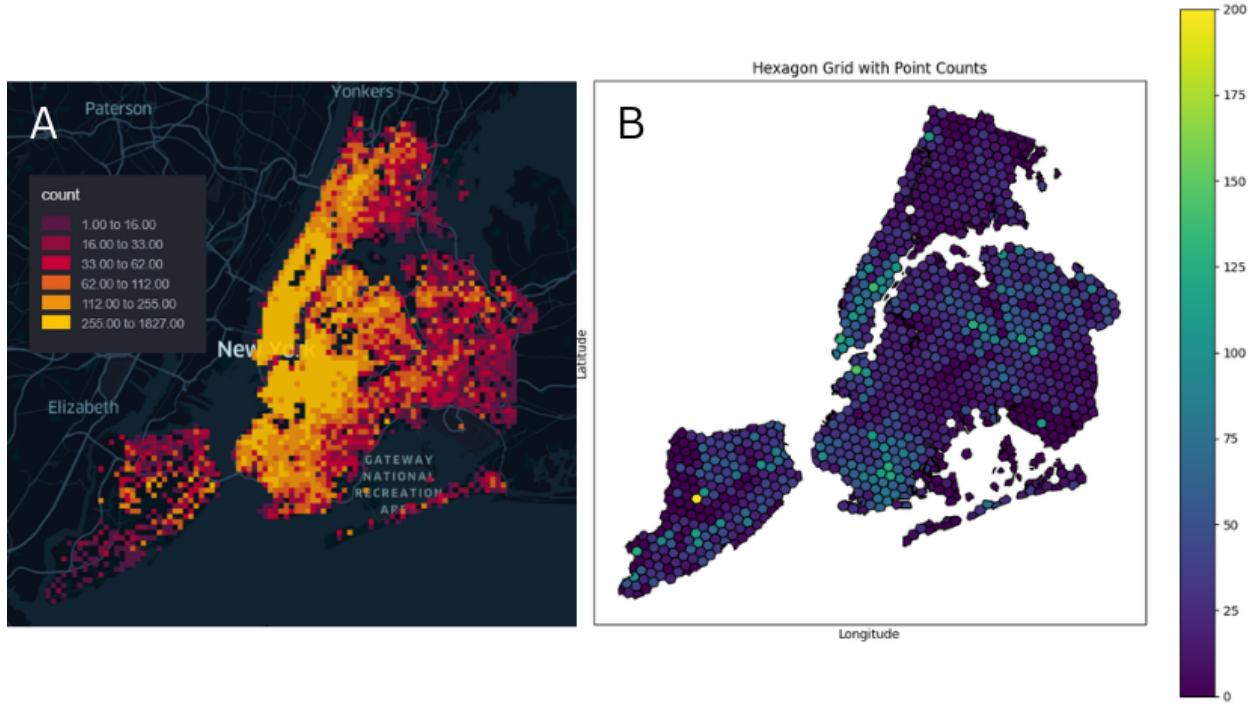


Figure 11. Visualization of EV Demands in New York City

Panel A: Thermal-style visualization with a legend indicating counts from 1 to over 1800, where red signifies the highest EV activity transitioning to yellow in regions with moderate activity. This panel effectively pinpoints the core zones of EV usage.

Panel B: Hexagon Grid with Point Counts, showing the distribution of EV activity across the city. Each hexagon's color intensity corresponds to the count of EVs, providing detailed insights into the spatial distribution patterns.

The hexagonal grid (Panel B) quantifies the concentration of EVs, where darker hexagons represent higher densities of EV usage, primarily centered around urban areas. The thermal map (Panel A) offers a qualitative view, using color intensities to highlight areas of intense EV activity, thus allowing for quick identification of high-demand zones.

4.4.3 CO2 Emission by Electric Vehicle

This step utilizes a replica travel dataset for New York City containing origin-destination trajectories. The data was filtered to include only trips where the primary mode was an electric vehicle (EV) and both the origin and destination were located within the New York City boundaries. This selective filtration ensures that the study's focus remains tightly bound to urban EV mobility patterns and their environmental implications.

1) Calculation of CO2 Emissions

The estimation of CO2 emissions from electric vehicles within the dataset was conducted using a robust formula that aligns with standards set by environmental agencies. The CO2 emissions for each electric vehicle trip were calculated using the following equation:

$$\text{CO2 Emissions} = \text{Distance Traveled} \times \text{CO2 Emission Factor}$$

The **Distance Traveled** was meticulously determined by mapping the shortest legal driving route between origin and destination coordinates. This was achieved using the OpenStreetMap (OSM) platform and the Open Source Routing Machine (OSRM), known for their reliability in delivering precise routing information. The **CO2 Emission Factor** for electric vehicles is set at 175 g CO2/km, a value recommended by the U.S. Environmental Protection Agency. This factor is derived from the average emissions associated with electricity generation sources in the region, reflecting the indirect emissions of EVs.

2) Spatial Distribution Analysis via Hexagonal Grid

For a granular spatial analysis, the study overlaid a hexagonal grid on the map of New York City using the H3 geospatial indexing system at resolution 8, which corresponds to hexagons with an edge length of approximately 492 meters. This fine resolution facilitates a detailed examination of emission distribution across diverse urban landscapes. To map emissions, three methods were tested for assigning emissions to hexes:

- i) Origin-Destination (OD): Total emissions divided evenly between origin and destination hexes.
- ii) Straight-line: LineString routes created between OD points, intersecting hexes identified, emissions divided evenly among intersected hexes.
- iii) Routing: Shortest driving routes obtained from Mapbox API, accounting for road network. Emissions are divided evenly among intersected hexes along the routes.

The initial approach to mapping CO2 emissions involved assigning the computed emissions to the hexagonal cells corresponding to the origin and destination points of each trip. This method, however, did

not reflect the true dispersion of emissions along the routes traveled. The routing method provides the highest fidelity representation by following actual driving paths rather than straight lines.

i) Route Simulation Using OpenStreetMap (OSM) Data

To approximate the actual travel path, each EV trip was mapped using the shortest legal driving route data obtained from OpenStreetMap. This step ensured that the CO₂ emissions were distributed across a realistic trajectory, enhancing the granularity of our emissions impact assessment. Utilizing the Mapbox Directions API, which is adept at handling large datasets, the shortest driving route for each trip was converted into a polyline. This polyline was then used to determine the set of H3 hexagons it traversed.

ii) Grid Overlay and Emissions Allocation

A spatial hexagonal grid was overlaid on the map of New York City, and the total CO₂ emissions for each trip were equitably distributed among the intersected hexagons. This distribution was proportionate to the number of hexes traversed by the route, offering a detailed view of emissions dispersion.

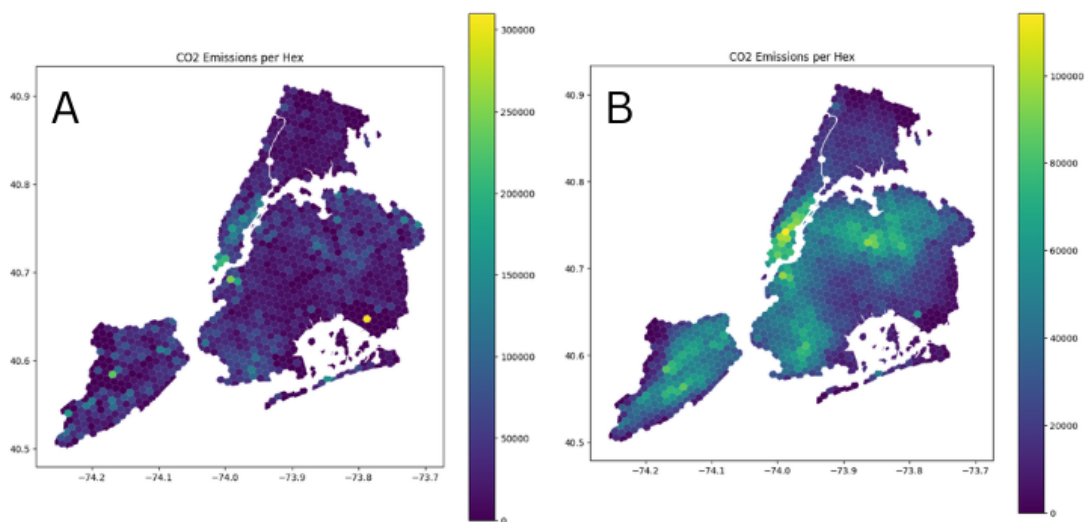


Figure 12. Spatial Distribution of CO₂ Emissions per Hex from Electric Vehicles in NYC

Figure 12 presents two subfigures (A and B) depicting the spatial distribution of CO₂ emissions per hexagonal grid cell from electric vehicles (EVs) in New York City, obtained using different methodologies. Subfigure A refers to Origin-Destination (OD) Distribution, it shows the CO₂ emissions assigned to each hex based on the origins and destinations of EV trips. The emissions are divided evenly between the origin and destination hexes containing the trip endpoints. The resulting pattern reveals hotspots around transportation hubs and dense urban areas, corresponding to higher EV trip volumes starting or ending in those locations. However, this OD approach oversimplifies the distribution by concentrating emissions at just the origin and destination points. In contrast, subfigure B (Straight-line

Distribution) depicts the emissions distribution using a straight-line methodology. For each trip, a LineString is constructed between the origin and destination, and the emissions are divided evenly among the intersected hexes along this straight line. Compared to the OD distribution, this approach results in a more dispersed pattern, with emissions distributed along paths between origins and destinations. Major transportation corridors become visible as linear features with higher emissions.

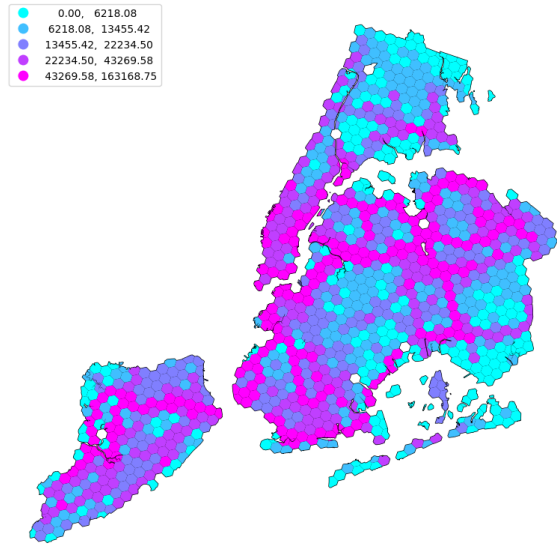


Figure 13. Spatial Distribution of CO2 Emissions Quantiles from EVs Using Routing Method

Figure 13 depicts the spatial distribution of CO2 emissions per hexagonal grid cell from electric vehicles (EVs) in New York City, obtained using the routing method. This method leverages the Mapbox Directions API to obtain the shortest driving routes between origin and destination coordinates, accounting for the actual road network constraints. It provides the most realistic representation by mapping emissions along actual driving routes on the road network obtained from Mapbox.

- High Emission Zones

The areas depicted in deep magenta indicate the highest quantiles of CO2 emissions. These zones likely correspond to areas with high EV traffic volumes, including major roads, intersections, and possibly areas with higher population densities or commercial activities. These zones are essential for targeting emissions reduction strategies, such as deploying more EV charging stations or optimizing traffic flow to reduce idling and congestion.

- Moderate to Low Emission Zones

Moving from deep magenta to lighter shades (pink and cyan), these areas represent moderate to lower emission quantiles. These might correspond to residential areas or less densely trafficked routes where EV

usage is lower or trips are shorter on average. Understanding these patterns can help in urban planning, such as improving access to public transit in these areas to maintain low emission levels.

- Lowest Emissions

The areas in light cyan reflect the lowest emissions, potentially indicating regions with minimal EV activity or highly efficient traffic conditions. These could be quieter residential neighborhoods or regions not typically frequented by commuter or commercial EV traffic.

- Spatial Trends and Urban Layout

The general distribution of colors across the map suggests a trend where central and more urbanized parts of the city have higher emissions, potentially due to higher EV utilization and denser traffic patterns. In contrast, peripheral areas appear to have lower emissions.

The spatial clustering of higher emission hexes corresponds with areas of potentially higher EV adoption, traffic volumes, and charging infrastructure demand. Lower emission areas may guide the strategic placement of charging stations to facilitate wider EV uptake. This fine-grained mapping enables correlational analysis with factors such as population density, road hierarchy, public transit access, and socioeconomic indicators to identify environmental justice considerations.

4.5 Mapping and Measuring Urban Structure Factor Using Osmnx

Apart from human traveling behavior and transportation mode, the urban construction environment can also generate an impact on the city's thermal environment and distribution of EV infrastructure. Here I considered 2 main aspects:

- Buildings in the city, especially focusing on high-rise buildings;
- Road network, analyzing topological features of driving roads.

4.5.1 Buildings Height Distribution

The construction of high-rise buildings requires a large amount of energy and resources, which will increase energy consumption and carbon emissions in cities and aggravate urban environmental pollution, thus potentially contributing to the urban heat island effect. Study shows that in the scope of building construction, the carbon emissions per unit area of the construction works of ultra-high-rise buildings amount to $0.402 \text{ tCO}_2\text{e/m}^2$, which is about 1.5 times higher than that of common multi-story buildings. On the other hand, high-rise buildings also have an influence on attracting more traffic flow, due to the dense economic activities it carries and thus increase the traffic demand, generating more trips. Therefore, building height is worthwhile to take into consideration when looking into heating, emission, and transportation issues.

1) Data processing

To further explore the relationship between buildings' height with other variables, I gained building footprint shapefile data through New York City Open Data, which represents the full perimeter outline of each building as viewed from directly above, as well as the centroid of each building. Additional attribute information maintained for each feature includes: Building Identification Number (BIN); Borough, Block, and Lot information(BBL); ground elevation at building base; roof height above ground elevation; construction year, and feature type. The centroids with geometry information make it easy to operate spatial join with other geographic layers. To edit them in Python, I converted them into a geodata frame, reading columns including 'ground elevation at building base', 'roof height above ground elevation', and geometry. To ensure that multiple layers are accurately matched, all geodata frame coordination reference systems are converted to 'EPSG:4326'.

2) Tools

The main library and packages I utilized during the process include: geopandas pandas and numpy, to deal with geodata frame, do spatial join and basic data processing and analyzing; Shapely, for manipulation and analysis of geometric objects; matplotlib, for map visualization.

3) Calculate the average building height per hexagon

After spatial join buildings geographic points using the inner join and 'within' option, buildings are By using 'groupby' with buildings height row and hex_id, I create groups where height rows with the same 'hex_id' value are placed together, then perform aggregation and calculate the average value of the height of every hex id. To further explore the distribution of building heights across different ranges, compute the height distribution using the value_counts function, which bins the height values into the specified number of ranges (here the study uses 25 as division). Then perform the normalization to ensure that the resulting counts are normalized to proportions.

4) Result Analysis

According to the table of distribution ranges, it can be seen that most of the buildings in New York are still kept below ten stories, and the super-tall buildings are mainly concentrated in the Manhattan area. This concentrated distribution of skyscrapers is also correlated with concentrated infrastructure investment and the distribution of traffic flows, reflecting the city's center of economic activity

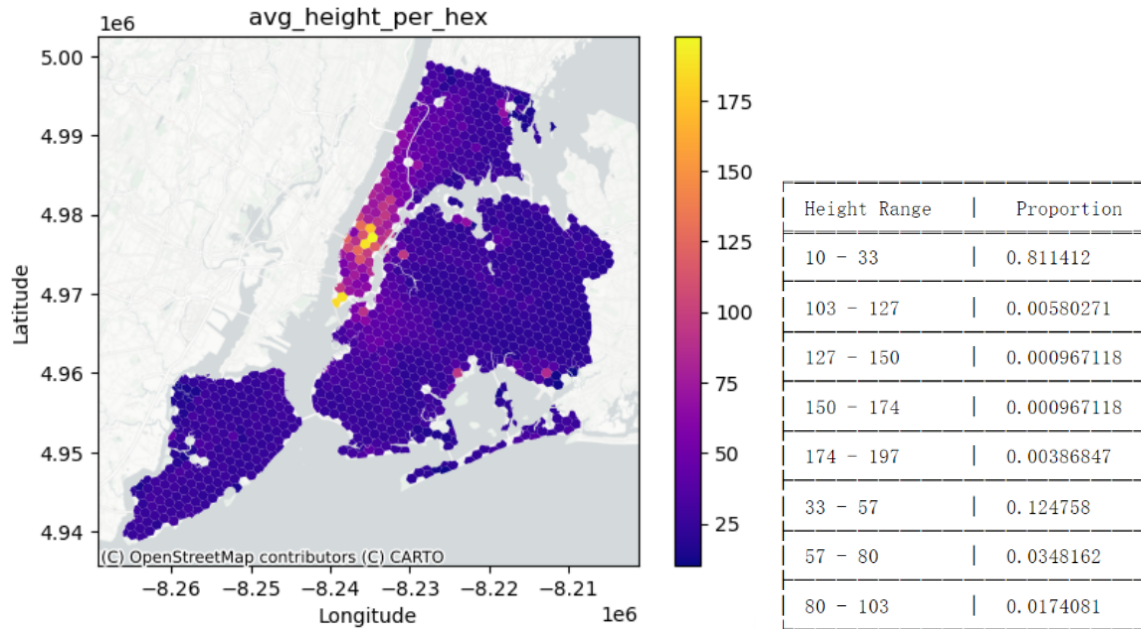


Figure 14. Spatial Distribution of Building Height

Table 2. Building Height Proportion

4.5.2 Road Network Structure

To get a better understanding of whether the road system's physical structure will relate to EV distribution and CO₂ emissions, I leveraged the OSMNX package to model the driving roads as the network. The road network is modeled as a directed primal graph, in which nodes in the network represent intersections in the roadway systems, while directed edges represent actual travelable road sections. Network topology stands on the foundation of the graph theory. A graph $G = (N, L)$ is a collection of n nodes ($N = \{1, 2, \dots, n\}$), which are interconnected by / links ($L = \{1, 2, \dots, l\}$). The study also selected Alameda County as a representative of the Bay Area. Since the study focuses on EVs and traffic, I selected only driving roads for the research object.

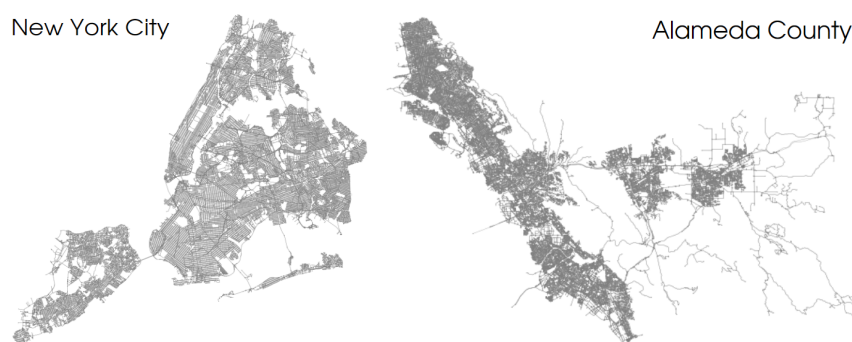


Figure 15. The road network of New York City and Alameda County

1) Overall Network: Basic information

The information on characteristics of the whole network can be gained from osmnx package by ‘ox.basic_stats’ demand. The stats information we get includes number of nodes, degree average, total edge length, average street density (km^2), etc. Here I select average degree, average edge length, intersection density, and street density as indicators for the level of being connected or compact:

- **k_average:** The average degree provides insights into the overall connectivity of a network. Networks with higher average degrees tend to be denser and more interconnected.
- **edge average length:** distances between nodes in the network. Networks with lower edge length averages tend to be more tightly connected or compact.
- **Intersection density:** the average number of intersections encountered along one kilometer of road.
- **Street length density:** the average length of streets per kilometer square within that area.

After gaining this information, the study utilized Matplotlib to plot two places together for comparison:

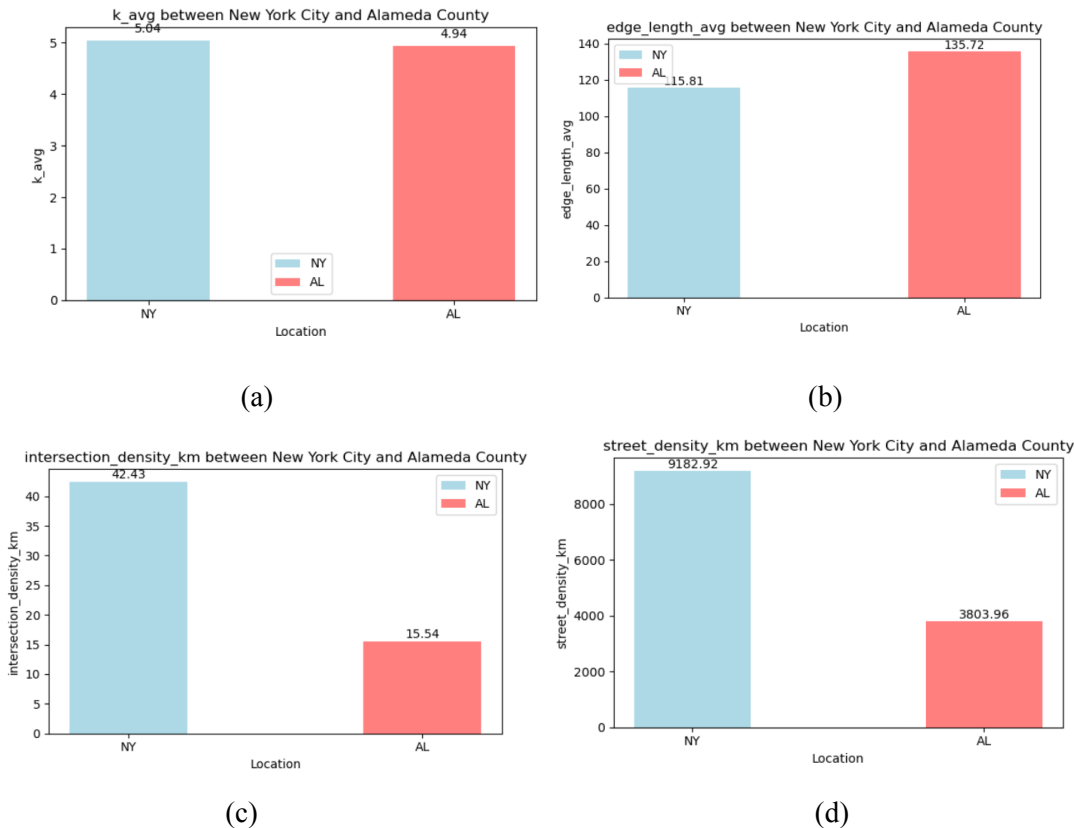


Figure 16. Comparison of Road Network in NYC and Alameda

(a): degree average (b): edge length average (c): intersection density (d): street density

Results indicate that New York City and Alameda county have relatively similar k degree and edge length. However, the intersection density in NY is way larger than that in Alameda, so the street length density reflects that NY has a very dense and connected road network.

2) Closeness/ Betweenness Centrality

To gain a more precise topological feature of the network, I also calculate the centrality value per hexagon. the closeness centrality measures how centrally located a node is. however, Because the calculation of betweenness centrality takes too much time and it's still in process, so I only presented closeness centrality here. The closeness centrality also can be directly obtained by the Network Science: nx package. The calculation behind is shown as Eq.(1):

$$C(v) = \frac{1}{\sum_{u \neq v} d(u,v)} \quad (1)$$

After the calculation, the centrality data is stored in a dictionary with node ID as the key. Through osmnx library, the study obtains the geographic coordinates and corresponding IDs of each point in the traffic network, which can assign the geographic coordinates to the centrality through the id connection, thus performing spatial join with hexagon and then calculating the average centrality per hexagon.

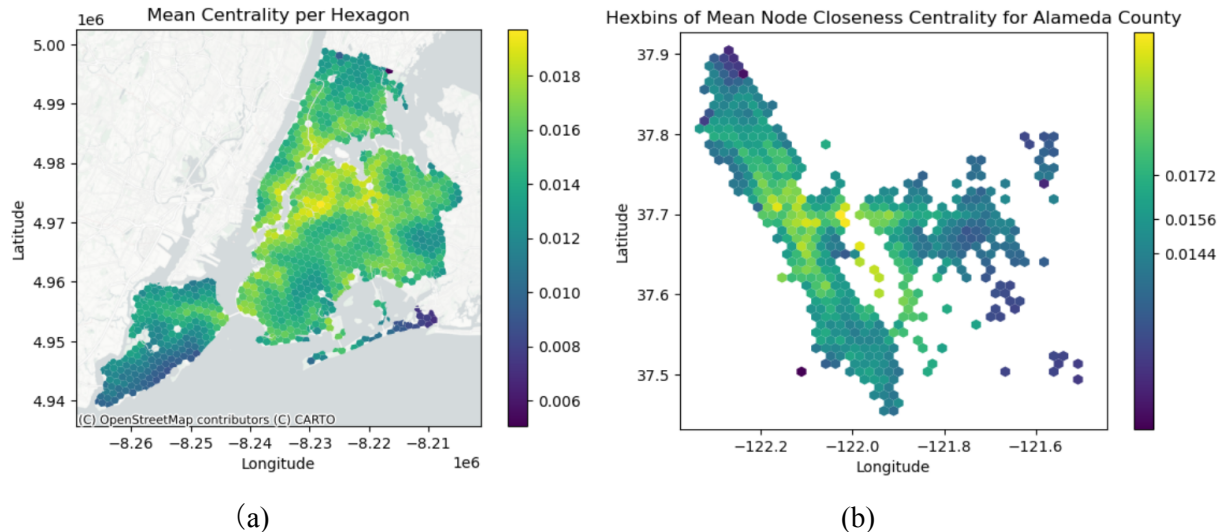


Figure 17. Average centrality distribution per hexagon: (a) NY City, (b) Alameda County

Since areas with high closeness centrality are often more accessible because they are closer to a large number of other locations in the network, as well as indicate where the hub is, these high-closeness centrality areas tend to have more transportation activities and other opportunities allocation, thus potentially contribute to attracting EV station allocation, on the other hand, contribute to higher emissions as well. The results show that the distribution of high centrality lies between Manhattan and Queen's

connections along the water, and also responds to the highway distribution pattern, indicating that most of the efficient transportation links and nodes are located here.

3) Average Degree/ Street Density

To get a more precise assessment of some features in a hexagon grid, I selected average node degree and street density to suggest the distribution of network connection and infrastructure intensity. The results showed that these two feature distributions are very similar.

The distribution visualization shows that there is a high-density road network distribution in the northern end of Queen, the area connected to Manhattan, and along the estuary in the southern end, as well as the north end. When looking at the land use of these dense streets area, most of them are residential neighborhoods, explaining the need for more density links and more connected intersections.

Also, it is worth noting that, from the visualized result, we can tell that the distribution of street or degree density has no correlation on the transportation hubs (closeness centrality).

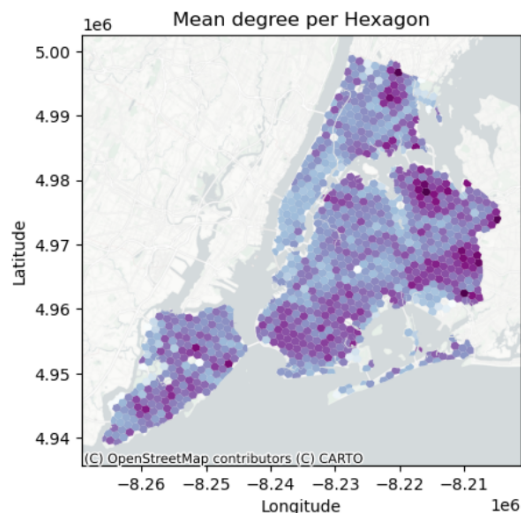


Figure 18. Distribution of Mean Degree

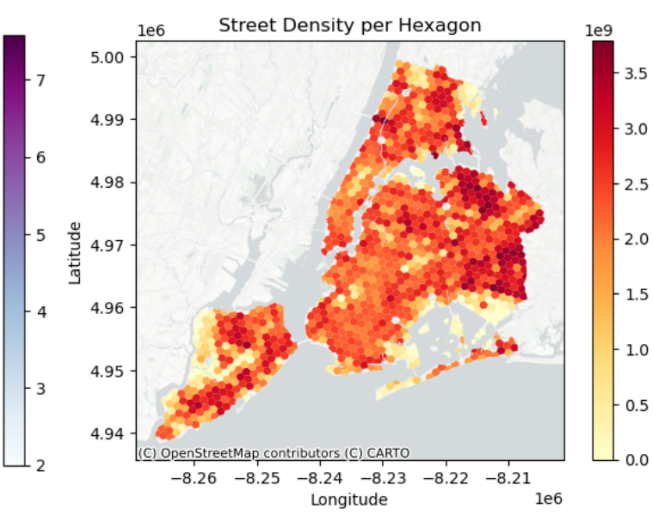


Figure 19. Distribution of Street Density

5. Correlation Analysis

To better understand the transportation insecurity characteristics of variables, the study analyzes various variables that influence the urban thermal environment and climate-related EV activity within New York City using a robust dataset partitioned into hexagonal grids. The correlation matrix, as depicted in Figure 20, illustrates the interrelationships among variables such as green space, EV station count, area, emissions per hex, EV demand count, mean centrality, mean degree, street density, and land surface temperature (lst_value).

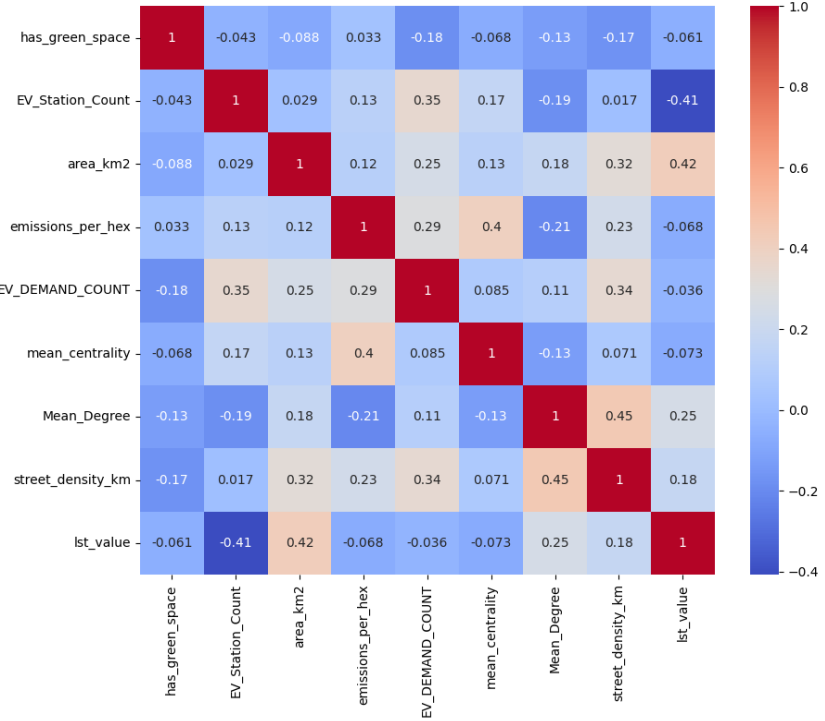


Figure 20. Correlation Matrix

5.1 Green Space and Urban Environment

The presence of green spaces (has_green_space) shows a moderate negative correlation with EV station count ($r = -0.043$), suggesting that areas with more green spaces may have fewer EV stations. This might reflect a divergence in urban planning priorities where recreational and ecological areas are less commercialized. However, green space exhibits a positive correlation with the area ($r = 0.42$), indicating that larger hexes are more likely to contain green spaces, potentially reflecting the distribution of parks and natural reserves which are typically situated in less densely built-up areas.

5.2 Electric Vehicle Infrastructure

Interestingly, the count of EV stations (EV_Station_Count) correlates strongly with the EV demand count ($r = 0.35$), signifying that areas with higher numbers of charging stations are likely to experience higher electric vehicle usage. This positive correlation underscores the critical role of infrastructure in supporting the adoption of electric vehicles, aligning with policy initiatives aimed at enhancing EV station accessibility to meet growing demand.

5.3 Urban Density and Emissions

Emissions per hex (emissions_per_hex) show a significant positive correlation with area ($r = 0.29$) and a moderate one with EV demand count ($r = 0.29$), suggesting that larger areas and those with higher EV activity tend to have higher emissions. This could reflect both increased vehicular activity and larger industrial or commercial spaces in these areas. Moreover, street density (street_density_km) is strongly correlated with mean degree ($r = 0.45$), indicating that more densely connected areas have greater road densities, which may contribute to higher traffic and subsequent emissions.

5.4 Thermal Environment

The lst_value, an indicator of land surface temperature, shows notable correlations with the area ($r = 0.42$) and emissions per hex ($r = 0.25$). These correlations might reflect the urban heat island effect where larger and more densely built-up areas exhibit higher surface temperatures due to human activities and reduced vegetative cover.

6. Principal Component Analysis

Principal Component Analysis (PCA) is a statistical technique utilized to reduce the dimensionality of large datasets while preserving as much variance as possible. In the context of mapping the urban thermal environment and the activity of electric vehicles (EVs) related to climate, PCA helps in identifying the principal components (PCs) that capture the significant variability in the environmental and activity-based data. This analysis forms a crucial part of understanding spatial patterns and underlying factors influencing the urban climate and EV dynamics.

6.1 Cumulative Explained Variance by PCA Components

The analysis begins with the determination of the number of components to retain, which is informed by the cumulative explained variance ratio depicted in Figure 21. The graph shows a steep increase in explained variance with the initial few components, suggesting that they capture the majority of the information in the dataset. The first three components account for approximately 60% of the variance, indicating significant underlying patterns in the data. Beyond the fifth component, the increments in explained variance become marginal, suggesting that these components contribute less to understanding the dataset.

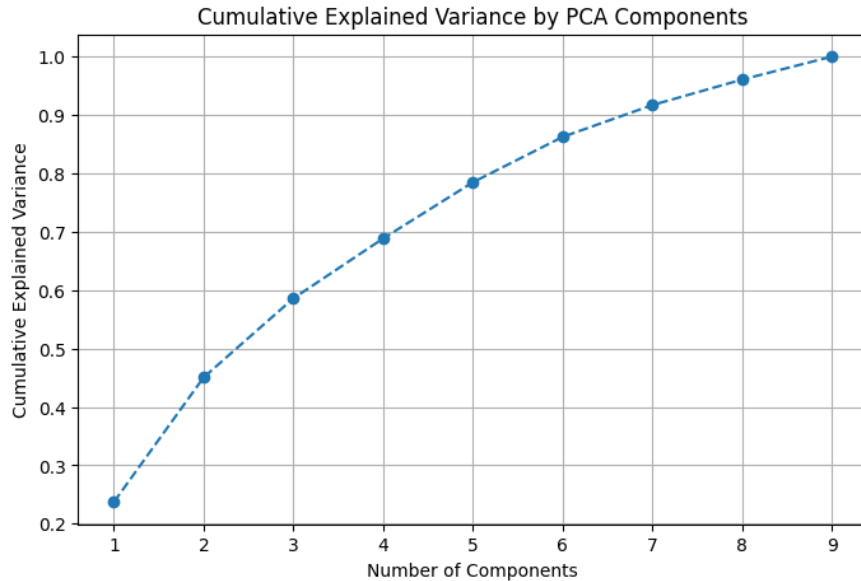


Figure 21. Cumulative Explained Variance by PCA Components

6.2 PCA Loadings and Component Interpretation

Table 3 presents the PCA loadings, which provide insights into the correlation between each of the original variables and the principal components. High loadings (both positive and negative) signify strong relationships with the respective components. For instance, if temperature and traffic volume have high positive loadings on the first component, this indicates that these variables fluctuate together across the dataset. Interpreting these loadings helps in hypothesizing about the environmental and operational dynamics captured by each component.

- PC1: Dominated by negative loadings on area_km2 and street_density_km, and a strong positive loading on has_green_space. This suggests that PC1 likely represents aspects of physical urban layout, where larger areas and denser streets contrast with the presence of green spaces.
- PC2: Characterized by significant positive loadings on EV_Station_Count, emissions_per_hex, and mean_centrality, implying that PC2 captures features related to the intensity of urban activities, including the availability of EV infrastructure and emission levels.
- PC3: Features opposing contributions from has_green_space, emissions_per_hex, and Mean_Degree, indicating it captures contrasting environmental impacts, possibly distinguishing between areas with natural cooling effects and those with higher pollution.
- PC4: Strongly influenced by has_green_space, suggesting a focus on regions with notable green coverage, which may affect local climates differently.

- PC5 to PC9: These components show mixed contributions from various factors, indicating more complex and subtle urban characteristics, such as specific local conditions or less dominant patterns in urban structure and environmental impact.

Table 3. PCA Loadings Table

	PC1	PC2	PC3	PC4	PC5	PC6	PC7	PC8	PC9
has_green_space	0.2422 38976	-0.001 299722	-0.328 952238	0.8685 89349	-0.066 37151	-0.196 340173	0.1468 52505	0.0422 65603	-0.1111 52493
EV_Station_Count	-0.044 968421	0.5072 00085	0.3649 26695	0.1457 61821	0.3365 3722	-0.344 921774	-0.1811 60999	0.4773 5384	0.3056 03645
area_km2	-0.460 002997	-0.077 905615	-0.246 740081	0.0985 86432	0.5579 0105	-0.248 819494	-0.278 940318	-0.508 794409	0.0434 03143
emissions_per_hex	-0.233 196042	0.4240 87222	-0.417 199802	0.0788 40311	-0.295 087303	0.4371 01917	-0.143 535118	-0.049 655378	0.5331 9375
EV_DEMAND_COUNT	-0.409 349776	0.2977 02592	0.2887 94584	0.1884 75709	0.1892 63064	0.3613 32995	0.6186 52165	-0.108 928392	-0.252 789609
mean_centrality	-0.1611 36317	0.3773 94468	-0.429 064432	-0.347 938921	-0.229 22293	-0.556 95296	0.3273 84565	0.0502 70571	-0.232 385862
Mean_Degree	-0.343 620858	-0.363 718705	0.3116 5257	0.1251 11818	-0.392 777729	-0.361 59915	0.2807 15845	-0.125 004034	0.5073 43507
street_density_km	-0.528 445388	-0.033 963124	0.1269 52228	0.1788 61462	-0.394 734411	0.0157 17616	-0.485 321965	0.2414 58695	-0.470 72463
lst_value	-0.287 146294	-0.438 553213	-0.378 073801	-0.064 35822	0.2924 96435	0.1332 33472	0.2072 56009	0.6486 05187	0.1057 69754

6.3 Explained Variance Ratio

Table 4 further details the percentage of variance explained by each principal component. This table is crucial for quantifying the importance of each component in the model. The explained variance ratios from Table 4 emphasize the importance of the first few components, with PC1 through PC5 explaining

nearly 80% of the total variance. This highlights that major urban characteristics are captured within these components, which include the physical layout, environmental infrastructure, and activity levels in the city.

Table 4. Explained PC Variance Ratio Table

Principal Component	Explained Variance Ratio	Cumulative Variance Explained
PC1	0.237294	0.237294
PC2	0.213356	0.450650
PC3	0.135297	0.585947
PC4	0.102573	0.688521
PC5	0.096218	0.784738
PC6	0.077674	0.862412
PC7	0.054580	0.916992
PC8	0.043621	0.960613
PC9	0.039387	1.000000

6.4 Elbow Method for Optimal Number of Components

Figure 22 employs the elbow method to visually determine the optimal number of PCA components. The plot shows a clear elbow at the third component, corroborating the analysis in Figure 21 that three to five components are sufficient to capture the essential structure of the data without significant information loss. The study adopts 4 clusters in the paper.

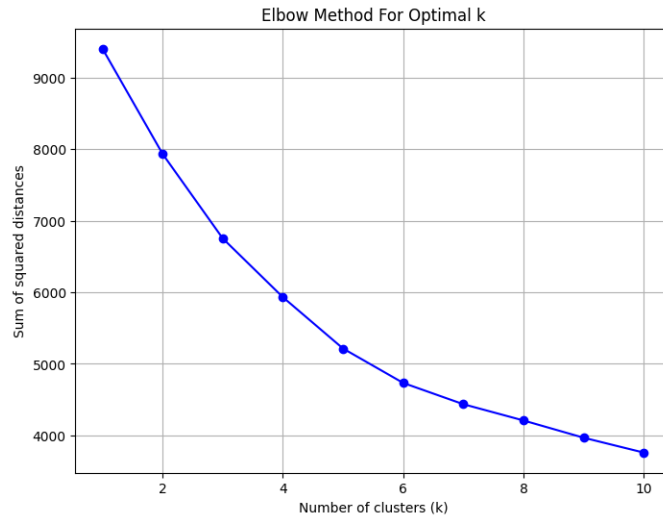


Figure 22. Elbow Method For Optimal K

6.5 Cluster Analysis on PCA Components

Figure 23 illustrates the cluster analysis performed on the PCA-reduced dataset. Each cluster represents a grouping of similar data points, suggesting common patterns across different segments of the urban environment. This clustering can be interpreted as different urban thermal profiles or EV activity patterns, which are critical for targeted environmental and transport policies.

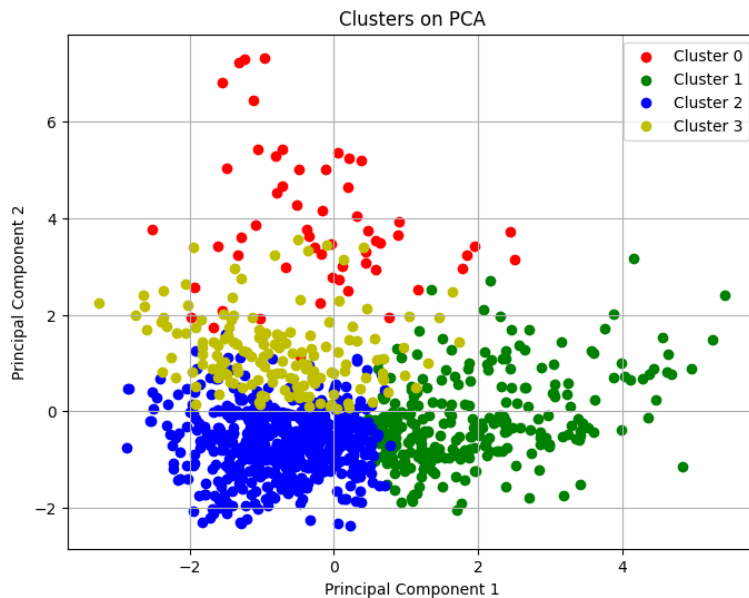


Figure 23. Clusters on PCA

6.6 Spatial Distribution of Clusters

Figure 24 shows the spatial distribution of PCA-based clusters across a hexagonal grid map of New York City. This visualization is instrumental in identifying geographical patterns and hotspots of thermal anomalies or high EV activity, which are vital for urban planning and climate adaptation strategies.

- Cluster 0 (Blue): This cluster might represent areas with higher green space presence, lower street density, and possibly lower overall urban activity, conducive to lower temperatures and reduced environmental impact. These could be more residential or peripheral areas.
- Cluster 1 (Pink): Likely to indicate regions with high EV infrastructure and possibly higher emissions, reflecting areas with substantial urban activity. These could be central or commercial areas where both the demand and supply for EVs are high.
- Cluster 2 (Cyan): This cluster could encompass zones with an intermediate mix of attributes, possibly suburban or transitioning areas with moderate levels of both green space and urban density.
- Cluster 3 (Red): Areas in this cluster may have less green space and higher street density, potentially correlating with higher local temperatures and greater urban congestion.

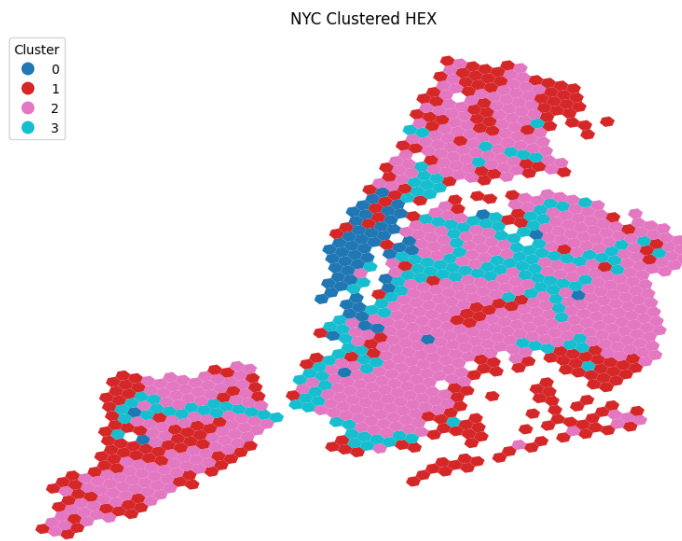


Figure 24. NYC Clustered Hexagon

The spatial distribution of these clusters on the hex map provides crucial insights into the urban thermal environment and EV activity across NYC. It allows urban planners and policymakers to identify specific areas that may require targeted interventions to manage heat islands or enhance EV infrastructure. This analysis also aids in understanding how urban planning and sustainability efforts can be directed to optimize the urban environment in response to climate challenges.

In summary, the PCA analysis reduces the complexity of the hexagon variable data but also reveals meaningful patterns and relationships, which are crucial for effective decision-making in urban environmental management and transportation planning. These findings are instrumental in guiding targeted interventions and enhancing the sustainability of urban areas in response to climate change.

7. Implication

7.1 Infrastructure Development

- **Increase charging stations to alleviate carbon emissions:** The mapping data can guide where to focus infrastructure improvements, such as adding more EV charging stations in high-emission areas to support increased EV use and potentially reduce emissions by facilitating more efficient vehicle use.
- **Integrate Green Spaces with EV Infrastructure:** The results show that green spaces and recreational parks in city lack of EV accessibility. City should plan for the strategic placement of EV charging stations near green spaces, contributing to eco-friendly connections with these spaces to promote the use of EVs, which can also make green spaces more accessible at the same time.
- **Expand EV Infrastructure:** The strong correlation between EV stations and EV demand indicates that infrastructure development is a key factor in the adoption of electric vehicles. City should raise investment in EV infrastructure, especially in areas with high EV demand. Increased infrastructure, in turn, can increase people's willingness to use electric vehicles, thereby increasing the demand for electric mobility.

7.2 Policy Making

- **Make targeted regulation:** Policymakers can use this detailed emissions mapping to craft targeted environmental regulations to encourage the use of EVs in higher-emission areas or to manage traffic in ways that could lower the overall emissions in congested areas.
- **Incentive the EV charging installation:** The government can provide incentives for residential and commercial property owners to install EV charging points, to improve the infrastructure supply. Meanwhile, explore innovative financing mechanisms to support the development of sustainable urban infrastructure.
- **Data-driven policy making:** Integrate climate data into urban planning during the policy-making process, to anticipate and adapt to thermal changes. Set indicators that integrated multi-criteria data to guide project assessment towards emission-reduction goal.

- **Facilitate EV Solutions:** Conduct policies that facilitate EV use, for example, implement smart charging systems that optimize charging times and reduce peak load on the grid.

7.3 Urban Planning

- **Optimization of EV Facility Layout:** Urban planners might use this data to assess the effectiveness of current urban layouts in facilitating efficient EV use and consider adjustments to road networks or developments to optimize for lower emissions. It is necessary to consider factors such as traffic flow, parking demand, and power grid capacity to optimize the site selection and distribution of charging stations.
- **Smart growth development:** Focus on creating compact, mixed-use urban spaces to reduce the need for travel and associated emissions. Meanwhile, reserve sufficient space in urban planning for the construction of charging stations and ensure that new residential and commercial areas are equipped with charging facilities.

8. Conclusion and Next Step

8.1 Conclusion

Based on the analysis, there are interesting trends that can be seen from all the different mapping results. The visual mapping representation of LST and EV data is a powerful tool for understanding the environmental impact of EVs in urban settings and can significantly influence decisions in urban development, traffic management, and environmental policy. The observed correlations offer insights into the complex interplay between urban planning, infrastructure development, and environmental management. The strong association between EV infrastructure and demand highlights the need for strategic placement of charging stations to foster greater adoption of electric vehicles, thereby potentially reducing urban emissions. Additionally, the influence of green space on thermal regulation and urban aesthetics underscores the importance of integrating ecological considerations in urban development to mitigate the urban heat island effect and enhance quality of life.

8.2 Next Step

8.2.1 Racial Density Distribution

When considering the distribution of race and ethnicity alongside temperature distribution, EV demand, and emissions, it's crucial to acknowledge the potential disparities in access to resources and environmental impacts across different demographic groups. Thus, it is worthwhile to explore whether the race density has correlations with other variables

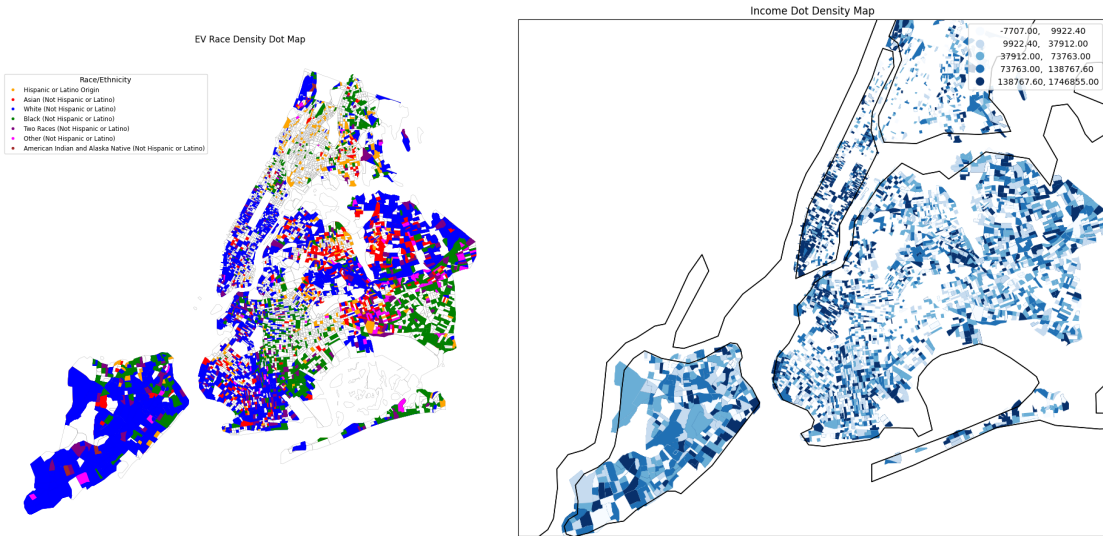


Figure 25. Racial Group (left) and Income Group (right) Distribution

8.2.2 Index Map

Based on the interested factors, we will also create 3 main scoring index map (heat influential factors) to overlay similar factors together in one map. they will be EV Acitivity map which contains EV stations, demand and emission factors, Urban structure map which contains urban construction environment and network; and Social Equity map which captures the race density.

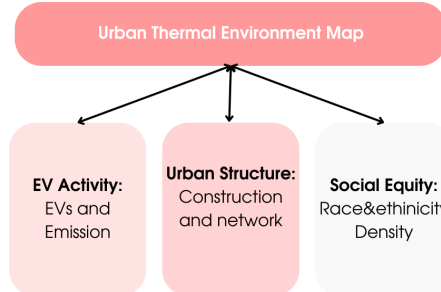


Figure 26. Index maps Illustration

The rationale and procedure of assigning scores is that:

- 1) Classify the values to several categories, and assign weight to categories. (eg: assign 3 to density of EV station bigger than 16 per hex)
- 2) Spatial Join separate hex data 1-1: on='hex_id', how='inner'.
- 3) Calculate the final cumulative score of each map, and visualize the final score

By overlaying similar factors onto a single map, we can perform a more integrated analysis that considers the multifaceted nature of urban issues. This holistic approach can lead to more effective and balanced policy decisions.

8.2.3 Deliverable

The study will also add a ArcGIS Story Map, the link will be put in the project GitHub page. The code and material used for this study can be found through the Github Page:

[Mapping-urban-thermal-environment-&-climate-related-EV-activity \(github.com\)](https://github.com)

Reference

Feng, T., Zhou, B. Impact of urban spatial structure elements on carbon emissions efficiency in growing megacities: the case of Chengdu. *Sci Rep* 13, 9939 (2023). <https://doi.org/10.1038/s41598-023-36575-6>.

ZHANG J 1, LI X 1, YANG Y 2. The impact of street network structure on carbon emissions from commuting: Evidence from three Chinese cities. Proceedings of the 13th Space Syntax Symposium. Published online 2022.

<https://www.hvl.no/globalassets/hvl-internett/arrangement/2022/13sss/340zhang.pdf/>.

Seonju Jang, Jinhyun Bae, YouJoung Kim, Street-level urban heat island mitigation: Assessing the cooling effect of green infrastructure using urban IoT sensor big data, *Sustainable Cities and Society*, Volume 100, 2024, 105007, ISSN 2210-6707.

<https://doi.org/10.1016/j.scs.2023.105007>.

Xiao, R., Wang, G. & Wang, M. Transportation Disadvantage and Neighborhood Sociodemographics: A Composite Indicator Approach to Examining Social Inequalities. *Soc Indic Res* 137, 29–43 (2018).

<https://doi.org/10.1007/s11205-017-1616-2>.

Revi, Aromar, David E Satterthwaite, Fernando Aragón-Durand, Jan Corfee-Morlot, and Robert B R Kiensi. “Coordinating Lead Authors” n.d.

Hardman, Scott, Amrit Chandan, Gil Tal, and Tom Turrentine. “The Effectiveness of Financial Purchase Incentives for Battery Electric Vehicles – A Review of the Evidence.” *Renewable and Sustainable Energy Reviews* 80 (December 1, 2017): 1100–1111. <https://doi.org/10.1016/j.rser.2017.05.255>.

Hsu, Angel, Jonas Tan, Yi Ming Ng, Wayne Toh, Regina Vanda, and Nihit Goyal. “Performance Determinants Show European Cities Are Delivering on Climate Mitigation.” *Nature Climate Change* 10, no. 11 (November 2020): 1015–22. <https://doi.org/10.1038/s41558-020-0879-9>.

Husni, Emir, Galang Adira Prayoga, Josua Dion Tamba, Yulia Retnowati, Fachri Imam Fauzandi, Rahadian Yusuf, and Bernardo Nugroho Yahya. “Microclimate Investigation of Vehicular Traffic on the Urban Heat Island through IoT-Based Device.” *Helyon* 8, no. 11 (November 2022): e11739.

<https://doi.org/10.1016/j.helyon.2022.e11739>.

Kammuang-Lue, Niti, Phrut Sakulchangsatjatai, Pisut Sangnum, and Pradit Terdtoon. "Influences of Population, Building, and Traffic Densities on Urban Heat Island Intensity in Chiang Mai City, Thailand." *Thermal Science* 19, no. suppl. 2 (2015): 445–55.

Li, Xiaoma, Yuyu Zhou, Sha Yu, Gensuo Jia, Huidong Li, and Wenliang Li. "Urban Heat Island Impacts on Building Energy Consumption: A Review of Approaches and Findings." *Energy* 174 (May 1, 2019): 407–19. <https://doi.org/10.1016/j.energy.2019.02.183>.

Liang, Xinyu, Shaojun Zhang, Ye Wu, Jia Xing, Xiaoyi He, K. Max Zhang, Shuxiao Wang, and Jiming Hao. "Air Quality and Health Benefits from Fleet Electrification in China." *Nature Sustainability* 2, no. 10 (October 2019): 962–71. <https://doi.org/10.1038/s41893-019-0398-8>.

Lin, Pingying, Stephen Siu Yu Lau, Hao Qin, and Zhonghua Gou. "Effects of Urban Planning Indicators on Urban Heat Island: A Case Study of Pocket Parks in High-Rise High-Density Environment." *Landscape and Urban Planning* 168 (December 1, 2017): 48–60. <https://doi.org/10.1016/j.landurbplan.2017.09.024>.

Lu, Jun, Chundie Li, Chuck Yu, Ming Jin, and Shaowei Dong. "Regression Analysis of the Relationship between Urban Heat Island Effect and Urban Canopy Characteristics in a Mountainous City, Chongqing." *Indoor and Built Environment* 21, no. 6 (December 1, 2012): 821–36. <https://doi.org/10.1177/1420326X12461659>.

Mussetti, Gianluca, Edouard L. Davin, Jonas Schwaab, Juan A. Acero, Jordan Ivanchev, Vivek Kumar Singh, Luxi Jin, and Sonia I. Seneviratne. "Do Electric Vehicles Mitigate Urban Heat? The Case of a Tropical City." *Frontiers in Environmental Science* 10 (February 18, 2022). <https://doi.org/10.3389/fenvs.2022.810342>.

Wolfram, Paul, and Nic Lutsey. "Electric Vehicles: Literature Review of Technology Costs and Carbon Emissions," n.d.

Yin, Chaohui, Man Yuan, Youpeng Lu, Yaping Huang, and Yanfang Liu. "Effects of Urban Form on the Urban Heat Island Effect Based on Spatial Regression Model." *Science of The Total Environment* 634 (September 1, 2018): 696–704. <https://doi.org/10.1016/j.scitotenv.2018.03.350>.